A Pipeline Approach to Developing Virtual Tests for Composite Materials

Brian Cox[1,*], Hrishikesh Bale[2], Matthew Blacklock[3], Bao-Chan Do[4], Renaud Rinaldi[3], Robert Ritchie[2], Qingda Yang[4], Frank Zok[3], and David Marshall[1]

[1] Teledyne Scientific Co LLC, Thousand Oaks, CA 91360, USA
[2] University of California, Berkeley, CA 94720, USA
[3] University of California, Santa Barbara, CA 93106, USA
[4] University of Miami, Coral Gables, FL 33124, USA
* Corresponding author: bcox@teledyne.com

Abstract A multi-disciplinary project combines experiments and theory to build high-fidelity virtual tests of composite materials. The virtual test is assembled via a "pipeline" running through a number of collaborating institutions. Key experimental challenges are acquiring 3D data that reveal the random microstructure and damage events at high temperatures in the interior of the composite with very high resolution (~ 1 μm). Key theoretical challenges include representing the stochastic characteristics of the 3D microstructure, modeling the failure events that evolve within it, and developing efficient methods for executing large ensembles of stochastic virtual tests. To begin, 3D images of 3D woven ceramic composites are captured by x-ray μCT on a synchrotron beamline. The statistics of the shape and positioning of the fiber tows in the 3D architecture are used to calibrate a generator that creates virtual specimens that are individually distinct but share the statistical characteristics of measured specimens. Failure of the virtual specimens is simulated by advanced computational methods, revealing the complete failure sequence of multiple interacting crack types. Validation of the analytical methods is performed by comparing with data captured at 1500°C and above, using digital image correlation or μCT to track damage evolution.

Keywords virtual test, stochastic, high temperature, ceramic, textile

1. Introduction

One role of a virtual test, as its name suggests, is to replace a real engineering test by a computer simulation. Ideally, the simulation would predict engineering properties *ab initio* with sufficient fidelity that the real test becomes unnecessary. More realistically, a virtual test calibrated by a few real tests will reduce the matrix of real tests needed to ensure safe use of a material, perhaps by an order of magnitude or more [1].

Of equal interest is the possibility that a virtual test can function as a tool for optimizing material design [1-5]. Indeed, a virtual test can yield much richer information about the correlation between the microstructure of a material and its performance than is easily available from experiments: in the virtual test, we have full knowledge of the microstructure and its effect on the details of failure mechanisms, whereas in the real test, such effects are often concealed in the interior of the specimen.

Virtual tests are of special value for high temperature materials, e.g., the current generation of integral textile ceramic matrix composites [6] with potential use temperatures ranging up to 1500ºC. While mechanisms of failure in composites that act at room temperature can be determined quite readily either by modern 3D imaging or by destructive sectioning following interruption of tests, mechanisms acting at high temperatures are much more difficult to probe. The virtual test offers the possibility of probing details of damage mechanisms for different temperature and loading histories using simulations coupled to relatively simple surface observations on real specimens. Nevertheless, advancing test methods applicable to high temperatures remains critical: the proven fidelity of a virtual test can never exceed the ability to identify the mechanisms that must be

modeled by direct experimentation.

In the case of virtual tests for continuous-fiber composites, including composites reinforced by laminated unidirectional fiber plies and textile preforms, the high resolution now available in 3D imaging systems is yielding details of the stochastic variability of plies and fiber tows and even of the spatial distribution of the individual fibers that populate the plies and tows; certain characteristics of textile geometry and tow deformation have been measured [7-9], as well as porosity [10] and its changes during processing steps [10, 11]. These and other studies have also addressed achieving feature definition in ceramic composites [12], which is often made difficult by low x-ray absorption contrast between the constituent materials. In recent work, fiber tows are made to stand out by imaging composites with partially formed matrices [13]. This allows detailed analysis of the statistics of geometrical variability in the fiber reinforcement. The geometrical variability of fiber deployment is a source of scatter in composite performance [14-19].

In the remainder of this article, the sequential steps of constructing a virtual test are described. Interesting prior literature includes virtual tests for textile ceramic composites using models that directly reproduce a stochastic microstructure from micrographs [20] (rather than using a virtual specimen generator as described below).

2. The stochastic characteristics of textile composites

The details of fiber tow shape in textile composite specimens somewhat larger than but comparable in size to a single unit cell (several mm) can be determined most satisfactorily using micron-resolution X-ray computed tomography (μCT) in a high-flux synchrotron beamline. Avoiding the difficulty of reconstructing 3D domains from 2D images of serial sections in micro-toming techniques, μCT data reveal comprehensive geometrical information on the fiber tow scale. Information at even smaller scales, down to 1 μm, concerning matrix voids, individual fibers, and fiber coatings can also be extracted but image artefacts can compromise interpretation. Typical images of a 3D woven carbon/SiC composite are shown in Fig. 1. (This material was fabricated with only enough matrix to rigidify the structure, which simplified identifying tow domains [13].)

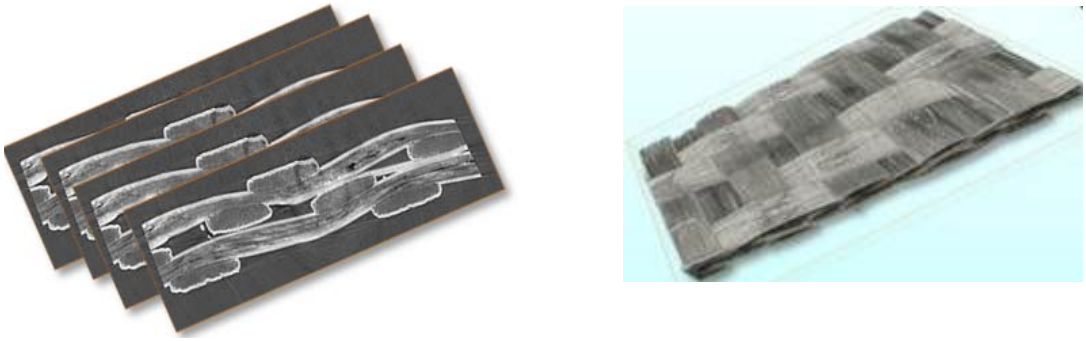

(a) (b)

Figure 1. μCT of a carbon/SiC woven composite, consisting of fiber tows coated by a thin layer of matrix material. (a) Image slices. (b) Re-constructed 3D image.

Fiber positioning variations can be decomposed into non-stochastic, periodic variations associated with the nominal periodicity in the textile architecture and stochastic deviations, which vary randomly though the fabric. A convenient and intuitively appealing treatment of the deviation divides it in turn into a superposition of “short-range” and “long-range” deviations. The

short-range deviations are those arising within a unit cell, referred to the center-of-mass of the unit cell, while the long-range deviations are the displacements of the centers-of-mass of unit cells over gauges much greater than the unit cell [13].

3. Virtual specimen generation

The art of formulating reconstruction algorithms or geometry generators for stochastic heterogeneous materials and related problems in statistical physics has a long history, mostly in the study of granular materials (e.g., [21, 22]. Textiles contrast with alloys in that they comprise long, continuous fiber bundles of essentially infinite aspect ratio, interlaced in complex but systematic patterns, a fact that calls for specialized algorithms in a virtual specimen generator, quite different in nature to those developed for statistically isotropic multi-phase materials (e.g., [23] and references therein).

The simplest geometry generator for a textile directly exploits the linear continuity of tows: a Markov Chain formulation generates fluctuations in any tow cross-sectional characteristic by marching systematically along the tow's length (Fig. 2) [24]. The key element of the Markov Chain is the Probability Transition Matrix (PTM), which determines the deviation and correlation length of any variable. The PTM is calibrated against measured statistical data, thus guaranteeing that the virtual specimens possess the same statistics as the real specimens that have been imaged. The Markov Chain formulation is very efficient and physically appropriate for the textile reconstruction problem, provided the dominant correlations are those along a tow, with correlations between tows relatively weak. It can be adapted to generate tows with 3D structure (Fig. 3) [25].

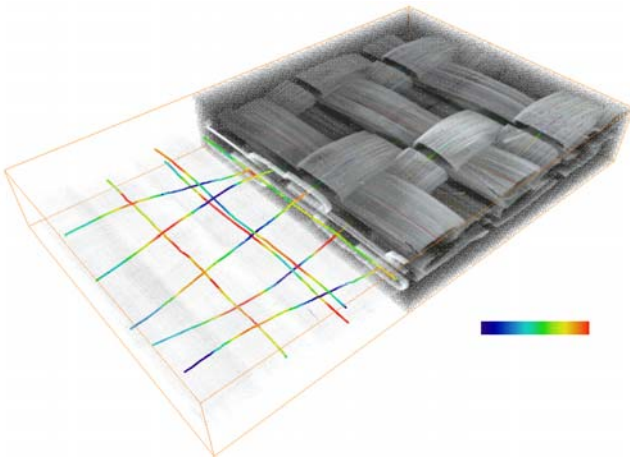

Figure 2. A μCT image yields statistics that are matched by generated virtual specimens. In this schematic, the generated tow structure at the left of the collage represents tows by 1D loci, suitable for use in the Binary Model [24, 26].

As it is described above, the Markov Chain formulation provides a purely empirical approach to virtual specimen generation: it simply matches statistical data from experiment. Models of the mechanics of fiber tow or preform deformation, which have been the basis for most other attempts to generate realistic geometric models of textiles, are not used. There is therefore no risk of errors flowing from uncertainty in the constitutive laws assumed to characterize such deformation, or in misrepresentation of the conditions during which preform fabrication or handling are carried out, including loading boundary conditions or the presence or absence of lubricating agents. The preform is analyzed as it is, in its final disposition.

However, an empirical approach has the disadvantage that the effects of changing processing conditions cannot be predicted. Such predictions are the province of mechanical models. An attractive future development will link mechanical modeling of preform deformation to empirical statistics, using the rich data content of detailed 3D measurements to calibrate and validate the mechanical model. The Markov Chain method may remain a useful tool within the linked super-model.

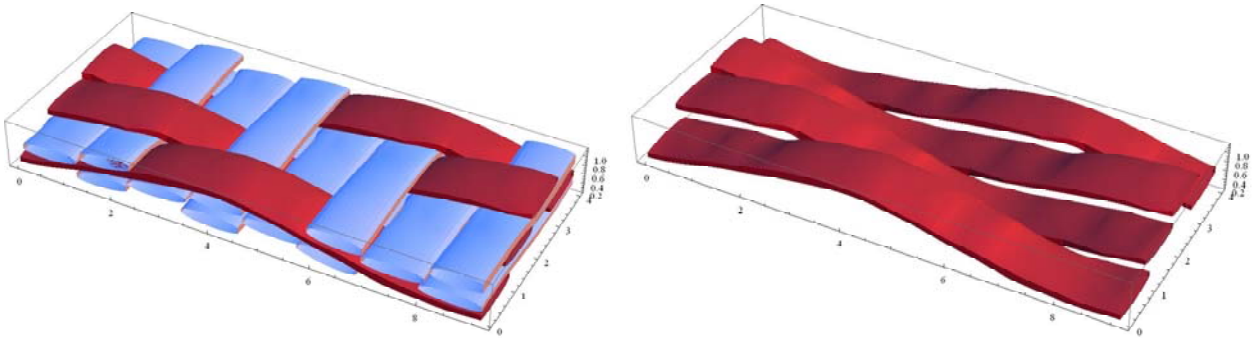

(a) (b)

Figure 3. The textile reinforcement of one virtual specimen generated with 3D tow representations using the Markov Chain method [25], showing (a) warp and weft tows together and (b) warp tows only. Tow shapes possess a combination of non-stochastic periodic variations (crimp features, etc.) and non-periodic stochastic deviations**.**

4. Observations of damage

The properties (strength, etc.) of a composite's constituent materials and their interfaces are generally unknown at high temperature. Phase properties cannot be calibrated by simple material tests, because the strength of different phases when they are juxtaposed at nm and μm scales is not represented by tests on large specimens of each phase isolated as a monolithic material. Tests are required on the composite materials themselves, executed at expected use conditions (i.e., temperatures of 1500ºC and higher), with sufficient resolution of mechanisms to enable the deduction of local material properties that control the mechanism. Direct observation of mechanisms is also critical to choosing correct formulations for simulations.

Measurements made at high temperature are the only faithful source of the details of failure. If a test specimen is cooled to an experimentally convenient 25°C for examination, the cooling itself introduces thermal strains of the order of at least 0.1–0.5% depending on composition and cooling rate, which can change the cracking patterns present before such cracks can be measured.

An apparatus was recently reported for acquiring 3D images via μCT of a specimen loaded in tension or compression at temperatures of 1500 – 1700°C in inert or oxidizing atmospheres (Fig. 4) [27]. Current maximum spatial resolution is 0.65 μm/voxel, yielding rich data on microstructure down to the fiber scale and μm-scale local failure mechanisms. Key data include variations of the opening displacements of fiber breaks and matrix microcracks as a function of load.

Data for a monotonic tension test of an angle interlock carbon-SiC woven composite specimens reveal different mechanisms of failure operating at 25°C and 1700°C (Fig. 5). At the lower resolution (1.3μm/voxel) used in these images, individual carbon fibers were not resolved. Nevertheless, the fiber tows are clearly distinguished from the matrix, which consists of a thin brighter layer of CVI SiC coating each tow and a polymer-derived SiC filling the remaining

occupied space. During initial loading at both temperatures, cracks formed in the matrix normal to the loading direction at positions where the matrix lay over a transverse fiber tow. With increasing load, the cracks grew through the transverse tows until they met an underlying axial tow (at loads in the range ~40 N to 70 N), where they were deflected. At 25°C this deflection involved formation of multiple splitting cracks (Fig. 5a), which progressed incrementally along the centers of the axial tows as the load was increased to the peak value of 150 N. Above 1600°C, the deflection of the crack at each tow involved a single crack that grew along the edge of the axial fiber tows as the load increased to 120 N (Fig. 5b), whereupon there was a large load drop. By influencing the access of ambient gas to the internal reinforcing fibers, differences in crack paths such as these could potentially have a large effect on subsequent high-temperature oxidation damage.

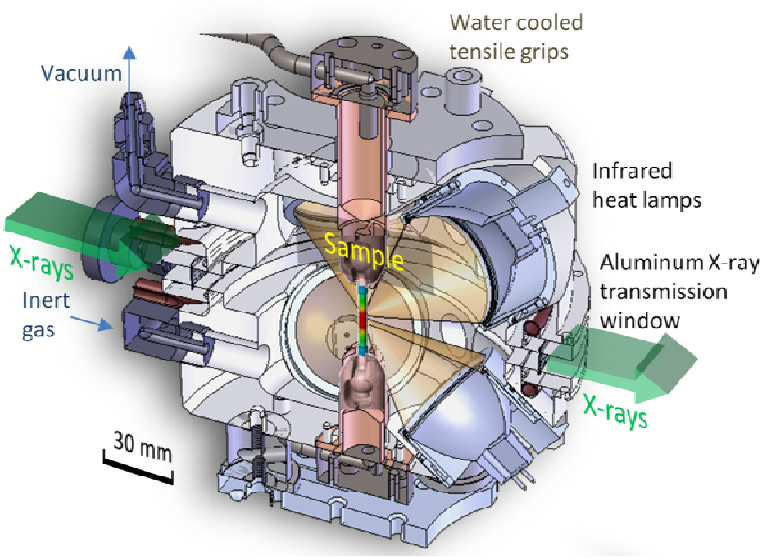

Figure 4. Sectional view of the heating chamber in a test rig designed to permit x-ray μCT imaging during testing at high temperature [27]. The x-ray beam passes through a load-supporting Al window, whose absorption is constant during rotations of the chamber and specimen and therefore does not impair image quality. The sample is held by water-cooled grips in the center of a sealed cell, which can be evacuated or filled with a selected gas. A hexapole arrangement of six 150 watt halogen lamps and reflectors gives a spherical hot zone of diameter ~5 mm.

5. Rapid computation of multiple discrete damage events

A critical element of high-fidelity simulations of failure is the ability to introduce new cracks during the execution of a simulation at locations and with orientation that are determined by the current local stress or strain fields. A major contribution to virtual test development has been the new formulation of finite elements (extended finite element method or X-FEM and others) that achieve this objective [28-32].

The augmented finite element method (A-FEM) [33, 34], similar in form to a conceptual element introduced earlier [29], has achieved detailed representations of generic multi-crack configurations and particularly high computational efficiency. Key attributes include: breakable elements that allow cracks to be introduced across which cohesive tractions exist, following a prescribed nonlinear fracture law; and breakable cohesive elements that allow the correct description of the local stress state around crack bifurcations or coalescence events (Fig. 6).

In addition to allowing correct description of key multiple crack configurations, the A-FEM incorporates a new iteration algorithm for searching for convergence in nonlinear problems, in which the global stiffness matrix is re-written in a piecewise linear form, allowing local convergence to be achieved in one or at most a few steps. The combination of A-FEM elements that use advanced quadrature algorithms and can be made somewhat larger than the length of the fracture process zone and the new iteration algorithm leads to gains in computational speed for typical nonlinear fracture problems of 2 – 3 orders of magnitude compared to standard methods such as X-FEM embedded in the ABAQUS commercial software [35]. As discussed further below, computational speed is essential in a virtual test strategy that seeks to address stochastic variability.

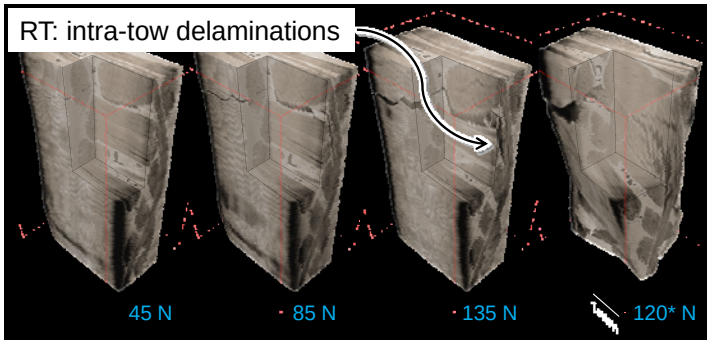

(a)

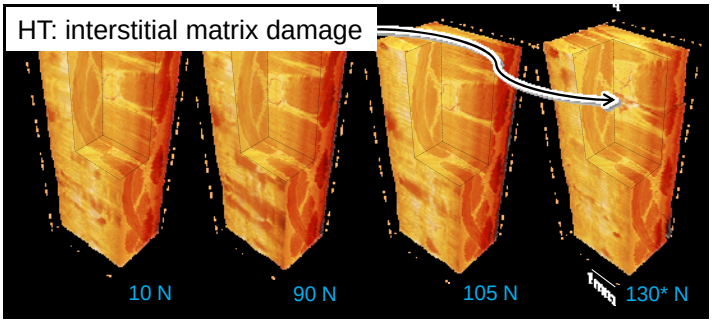

(b)

Figure 5. Internal damage in a C-SiC composite with textile-based carbon fiber reinforcements under tensile load at (a) 25°C and (b) 1600°C.

6. Monte Carlo methods vs. probabilistic theories

The Monte Carlo method using ensembles of stochastic virtual specimens provides the closest analogue of a real test matrix: a statistically significant number of virtual specimens are subjected to the same virtual test (or matrix of tests) and engineering predictions are deduced from the mean and scatter in the outcomes [36, 37]. Each specimen in the tested ensemble is one instance of a random microstructure that has been constructed by feeding pseudo-random numbers into calibrated distribution functions (a Monte Carlo procedure). The variance of the microstructure in the ensemble of virtual specimens is a major source of variance in predictions. With trivial modification, the load can also be made random, e.g., to simulate random overloads in a duty cycle.

Once a stochastic virtual specimen generator has been developed and constitutive laws have been calibrated, executing a Monte Carlo analysis is straightforward. Simulations are executed in sequence and predicted metrics (strength, strain to failure, etc.) are analyzed using the same statistical methods used to analyze real tests.

The computational expense of Monte Carlo analysis can be high. The uncertainty in a predicted mean property, such as the expected strength in a distribution of strengths, will fall as the number of computed cases N rises. If σ denotes the uncertainty in a predicted mean property normalized by the width of the distribution of the property, $\sigma \approx N^{-1/2}$. For example, if strength is predicted to have a deviance of 10%, then determining the mean strength to 1% accuracy requires 100 simulations.

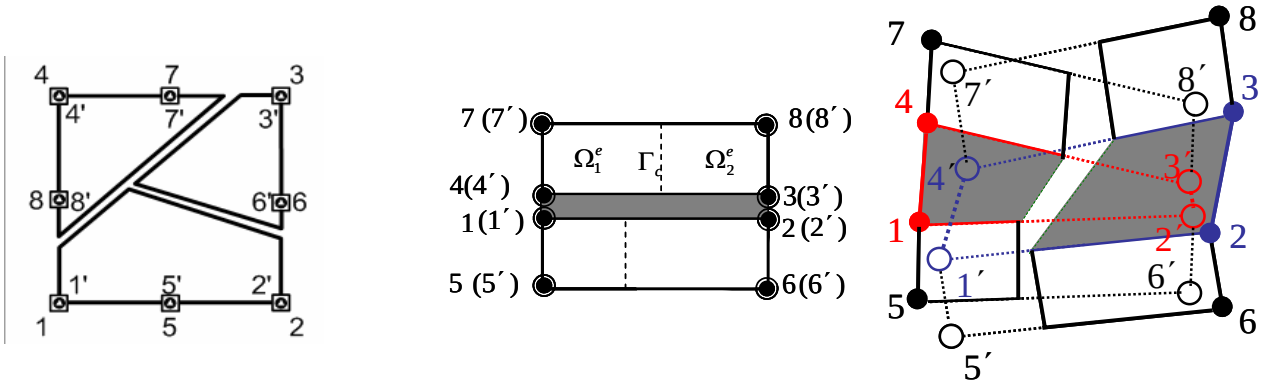

(a) (b)

Figure 6. (a) In the A-FEM formulation, a single element can split into several domains, accommodating a crack bifurcation event. (b) When a crack in a solid element impinges upon a material interface, the cohesive element governing fracture of the interface (grey domain, with width exaggerated for visibility) divides into two sub-elements, allowing the correct sign and magnitude of interfacial shear displacement to be computed on either side of the impinging crack.

If the virtual test is used in materials design, a design optimization study addressing the statistics of failure might require computing the effects of 10^2 – 10^4 different material or architectural parameters. To establish reasonably accurate trends in mean strength, 10^4 – 10^6 virtual tests must be executed. For the computational time to remain within one week (10^6 seconds) for a relatively wide search, a single virtual test should execute in 1 sec, to order of magnitude. Current execution times for multiple crack evolution leading to ultimate failure in a single virtual test are orders of magnitude higher than this.

Probabilistic models offer computational efficiency and the possibility of accurate predictions of rare events. In a probabilistic theory, instead of tracking damage evolution through a particular microstructure, one tracks the evolution of a probability distribution $P(X)$ for a damage variable X through time or elapsed fatigue cycles. Because $P(X)$ can be represented numerically with arbitrary precision over all values of X, accuracy in predicting the tails of the distribution is at least possible. However, is it not assured: accuracy also demands that the probabilistic theory incorporate a faithful representation of the details of the influence of the stochastic microstructure on the evolution of $P(X)$.

The first and simplest approach uses diffusion equations or discrete chain models to describe the evolution of a damage variable such as crack length, coupled to a simplified representation of the influence of some other factor, which could be a microstructural factor. However, such phenomenological models are limited in the degree of fidelity they can achieve in predicting the effects of microstructural variation within a single class of materials. They must use calibration data for the same materials as those for which predictions are to be made, with the same failure mechanisms and microstructural statistics being present. They cannot be used easily to make

predictions for materials with different microstructural statistics or different loading conditions. Improved fidelity requires incorporation of the details of how microstructure controls the evolution of local damage events.

A formulation that can improve fidelity in a probabilistic framework was presented by Pardee and colleagues [38, 39]. The Pardee formulation recognizes the discontinuous nature of crack growth by associating each of the three phases of damage development in the example of Fig. 7 with a distinct domain Ω_I, Ω_{II}, or Ω_{III} in the space in which probability density is defined. Thus, at a point in Ω_I one defines the probability density $P_I(X_I = a/D; t)da$ that a crack of length $X_I D \le a \le X_I D + da$ with $X_I < 1$ is propagating through the matrix at time t; at a point in Ω_{II} one defines the probability density $P_{II}(X_{II} = \beta; t)d\beta$ that an arrested crack has damage parameter $X_{II} \le \beta \le X_{II} + d\beta$ at time t; and at a point in Ω_{III} one defines the probability density $P_{III}(X_{III} = a; t)da$ that a crack of length $X_{III} \le a \le X_{III} + da$ with $X_I > 1$ is propagating into the fiber tow at time t.

With growth laws predicted by a small number of virtual tests and statistical distributions calibrated by experiments, the Pardee problem can be solved to generate rapid predictions of the full distribution function for engineering properties, such as the time to failure of the reinforcing tow in Fig. 7. Serving within such an efficient formulation, virtual tests can relate the statistics of rare failure events to microstructural variance with the least possible computational effort.

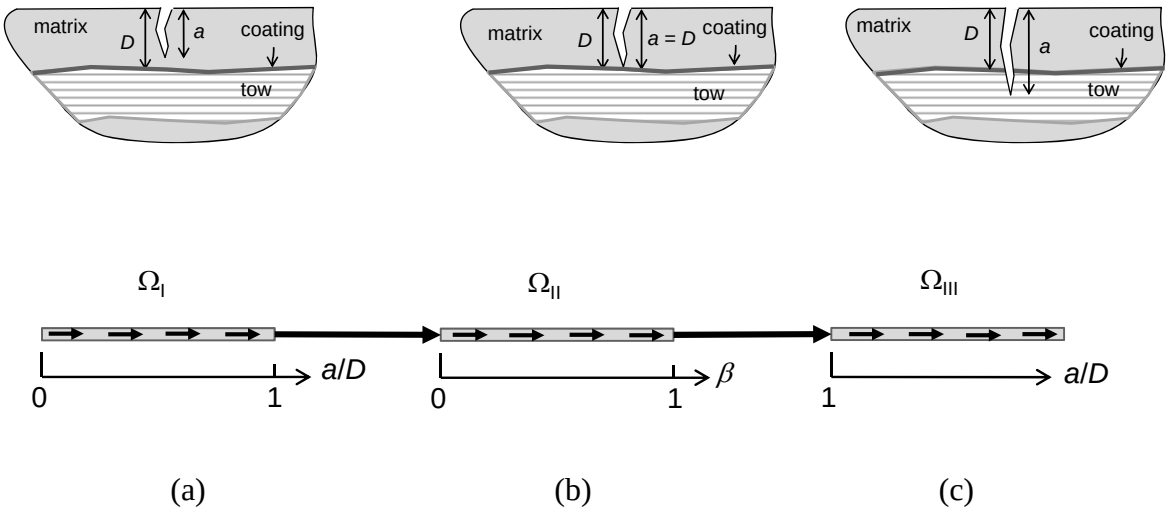

(a) (b) (c)

Figure 7. A microcrack (a) originating in a superficial matrix layer might (b) arrest temporarily at a fracture resistant coating that protects a tow before (c) propagating into the tow and exposing the fibers in the tow to the environment. In correspondence with the three stages of microcrack growth, there exist three domains Ω_I, Ω_{II}, and Ω_{III}, through which probability density flows in conservation equations describing their evolution; density flux is indicated by arrows. In domains I and III, the state variable is crack length a, while in domain II it is a damage parameter β that increases with time from 0 to unity.

References

1. Cox, B.N. and Q.D. Yang, *In quest of virtual tests for structural composites.* Science, 2006. **314**: p. 1102-1107.
2. Ashby, M.F., *Physical modelling of materials problems.* Materials Science and Technology, 1992. **8**: p. 102-111.
3. Llorca, J., et al., *Multiscale modeling of composite materials: a roadmap towards virtual testing.*

Advanced Materials, 2011. **23**: p. 5130-5147.
4. Pollock, T.M., et al., *Integrated computational materials engineering: A transformational discipline for improved competitiveness and national security.* 2008, National Research Council of the National Academies: Washington, D.C.
5. Evans, A.G., *Design and life prediction issues for high temperature engineering ceramic and their composites.* Acta Materialia, 1997. **45**: p. 23-40.
6. Marshall, D.B. and B.N. Cox, *Integral textile ceramic structures.* Annual Review of Materials Research, 2008. **38**: p. 425-443.
7. Badel, P., et al., *Simulation and tomography analysis of textile composite reinforcement deformation at the mesoscopic scale.* Composites Science and Technology, 2008. **68**: p. 2433-2440.
8. Desplentere, F., et al., *Micro-CT characterization of variability in 3D textile architecture.* Composite Science and Technology, 2005. **65**: p. 1920-1930.
9. Mahadik, Y., K.A. Robson Brown, and S.R. Hallett, *Characterisation of 3D woven composite internal architecture and effect of compaction.* Composites, Part A, 2010. **41**: p. 872-880.
10. Lee, S.-B., et al., *Pore geometry in woven fiber structures: 0/90 plain-weave cloth layup preform.* Journal of Materials Research, 1998. **13**(5): p. 1209-1217.
11. Kinney, J.H., et al., *X-ray tomographic study of chemical vapor infiltration processing of ceramic composites.* Science, 1993. **260**: p. 789-792.
12. Coindreau, O., G. Vignoles, and P. Cloetens, *Direct 3D microscale imaging of carbon-carbon composites with computed holotomography.* Nuclear Instruments and Methods in Physics Research B, 2003. **200**: p. 308-314.
13. Bale, H., et al., *Characterizing Three-Dimensional Textile Ceramic Composites using Synchrotron X-Ray Micro-Computed-Tomography.* Journal of the American Ceramic Society, 2011. **95**(1): p. 392-402.
14. Argon, A.S., *Fracture of composites*. Treatise of Materials Sciences and Technolgy. Vol. 1. 1972, New York: Academic Press.
15. Budiansky, B., *Micromechanics.* Composite Structures, 1983. **16**(1): p. 3-12.
16. Cox, B.N., et al., *Mechanisms of compressive failure in 3D composites.* Acta Metallurgica et Materialia, 1992. **40**: p. 3285-3298.
17. Fleck, N.A. and B. Budiansky, *Compressive failure of fibre composites due to microbuckling*, in *Inelastic Deformation of Composite Materials*, G.J. Dvorak, Editor. 1991, Springer-Verlag: New York. p. 235-274.
18. Fleck, N.A. and J.Y. Shu, *Microbuckle initiation in fibre composites: a finite element study.* Journal of the Mechanics and Physics of Solids, 1995. **43**(12): p. 1887-1918.
19. Marshall, D.B., et al., *Transverse strengths and failure mechanisms in Ti3Al matrix composites.* Acta Metallurgica et Materialia, 1994. **42**: p. 2657-2673.
20. Pineau, P., G. Couegnat, and J. Lamon, *Virtual testing applied to transverse multiple cracking of tows in woven ceramic composites.* Mechanics Research Communications, 2011. **38**(8): p. 7.
21. Cox, B.N. and W.L. Morris, *Monte Carlo simulations of the growth of small fatigue cracks.* Engineering Fracture Mechanics, 1988. **31**: p. 591-610.
22. Groeber, M., et al., *A framework for automated analysis and simulation of 3D polycrystalline microstructures. Part 2: Synthetic structure generation.* Acta Materialia, 2008. **56**: p. 1274-1287.
23. Jiao, Y., F.H. Stillinger, and S. Torquato, *A superior descriptor of random textures and its predictive capacity.* Proceedings of the National Academy of Science of the USA, 2009. **106**(42):

p. 17634-17639.
24. Blacklock, M., et al., *Generating virtual textile composite specimens using statistical data from micro-computed tomography: 1D tow representations for the Binary Model.* Journal of the Mechanics and Physics of Solids, 2012. **60**: p. 451-470.
25. Rinaldi, R., et al., *Generating virtual textile composite specimens using statistical data from micro-computed tomography: 3D tow representations.* Journal of the Mechanics and Physics of Solids, 2011. **in press**.
26. Cox, B.N., W.C. Carter, and N.A. Fleck, *A Binary Model of textile composites: I Formulation.* Acta Metallurgica et Materialia, 1994. **42**: p. 3463-3479.
27. Bale, H.A., et al., *Real-Time Quantitative Imaging of Failure Events in Ultrahigh-Temperature Materials under Load at Unprecedented Temperatures above 1700°C.* Nature Materials, 2012. **in press**.
28. Zi, G. and T. Belytschko, *New crack-tip elements for XFEM and applications to cohesive cracks.* International Journal for Numerical Methods in Engineering, 2003. **57**: p. 2221-2240.
29. Hansbo, A. and P. Hansbo, *A finite element method for the simulation of strong and weak discontinuities in solid mechanics.* Computational Methods in Applied Mechanics and Engineering, 2004. **193**: p. 3523-3540.
30. Andersson, T. and U. Stigh, *The stress–elongation relation for an adhesive layer loaded in peel using equilibrium of energetic forces.* International Journal of Solids and Structures, 2004. **41**(2): p. 413-434.
31. Moës, N., J. Dolbow, and T. Belytschko, *A finite element method for crack growth without remeshing.* International Journal for Numerical Methods in Engineering, 1999. **46**: p. 131-150.
32. Strouboulis, T., K. Copps, and I. Babuška, *The generalized finite element method.* Computational Mechanics Advances, 2001. **190**: p. 4801-4193.
33. Fang, X.J., et al., *An augmented cohesive zone element for arbitrary crack coalescence and bifurcation in heterogeneous materials.* International Journal of Numerical Methods in Engineering, 2011. **88**: p. 841-861.
34. Ling, D., Q. Yang, and B.N. Cox, *An augmented finite element method for modeling arbitrary discontinuities in composite materials.* International Journal of Fracture, 2009. **156**: p. 53-73.
35. Liu, W., et al., *An Accurate and Efficient Augmented Finite Element Method for Arbitrary Crack Interactions.* Journal of Applied Mechanics, 2012. **in press**.
36. Metropolis, N. and S. Ulam, *The Monte Carlo method.* Journal of the American Statistical Association, 1949. **44**: p. 335-341.
37. Cox, B.N., *Inductions from Monte Carlo simulations of small fatigue cracks.* Engineering Fracture Mechanics, 1989. **33**: p. 655-670.
38. Cox, B.N., W.J. Pardee, and W.L. Morris, *A statistical model of intermittent short fatigue crack growth.* Fatigue and Fracture of Engineering Materials and Structures, 1987. **9**(6): p. 435-455.
39. Pardee, W.J., et al., *Statistical Mechanics of Early Growth of Fatigue Cracks,* in *2nd Int. Symp. on Defects, Fracture and Fatigue*. 1982: Mont Gabriel, Canada. p. 99-111.

Acknowledgments

This work was supported by the Air Force Office of Scientific Research (Dr. Ali Sayir) and NASA (Dr. Anthony Calomino) under the National Hypersonic Science Center for Materials and Structures (AFOSR Contract No. FA9550-09-1-0477). We acknowledge the use of data from the x-ray synchrotron micro-tomography beam line (8.3.2) at the Advanced Light Source (ALS) at the Lawrence Berkeley National Laboratory (US Dept. of Energy, contract No. DE AC02 05CH11231).